UNITED STATES
DEPARTMENT OF THE INTERIOR
GEOLOGICAL SURVEY

INTERAGENCY REPORT: ASTROGEOLOGY 12

THE USE OF SPECTRAL ANALYSIS IN DESCRIBING LUNAR SURFACE ROUGHNESS

By

Wesley Rozema

December 1968

Prepared for the National Aeronautics and Space Administration (NASA) under Purchase Order No. W-12,388, Amend. No. 2

This report is preliminary and has not been edited or reviewed for conformity with U.S. Geological Survey standards and nomenclature.

Prepared by the Geological Survey for the National Aeronautics and Space Administration

INTERAGENCY REPORT: ASTROGEOLOGY 12

THE USE OF SPECTRAL ANALYSIS IN DESCRIBING LUNAR SURFACE ROUGHNESS

By

Wesley Rozema

December 1968

Prepared for the National Aeronautics and Space Administration (NASA) under Purchase Order No. W-12,388, Amend. No. 2

CONTENTS

ILLUSTRATIONS

TABLES

THE USE OF SPECTRAL ANALYSIS IN DESCRIBING LUNAR SURFACE ROUGHNESS

By Wesley J. Rozema

ABSTRACT

The power spectral density (PSD) function has been investigated in recent years as a means of statistically describing land-surface roughness. Knowledge of the PSD functions of lunar topographic profiles is useful for analyzing the manner in which experimental lunar roving vehicles will respond to lunar terrain. In addition, the function enables comparison of the relative "roughness" of different types of terrain.

Certain statistical problems are inherent in the determination of the PSD function. Methods of determining the function were selected and applied consistently to several terrestrial and lunar topographic profiles. Superposition of the graphs of these functions provides an intuitive comparison of the "roughness" of terrestrial and lunar terrains.

INTRODUCTION

The determination of a statistical description of the roughness of the lunar surface is vital for the design of lunar roving vehicles. Under the sponsorship of NASA, Mason, McCombs, and Cramblit (1964) and Olivier and Valentine (1965) proposed the ELMS and ELMO, respectively, as statistical models of the lunar surface. Schloss (1965) suggested the use of curvature as a surface roughness characteristic.

Efforts toward generating a statistical description of the roughness of the lunar surface were begun for the U.S. Geological Survey by McCauley (1964). Using data derived photometrically from Earth-based photographs, Rowan and McCauley (1965) found the mean and standard deviation of slopes to be useful statistical parameters for the quantitative description of lunar surface roughness at Earth-based resolutions. However, when considering the design of a lunar roving vehicle, neither the aforementioned parameters nor data from the maximum-resolution Earth-based lunar photographs are completely adequate.

At present, lunar surface features as small as 0.6 meter can be resolved through photoclinometric reduction of Lunar Orbiter II

and III photography. This degree of resolution is sufficient for lunar trafficability analysis. Furthermore, the power spectral density (PSD) function of a topographic profile has been found to be an especially useful statistic in the analysis of vehicular response to terrain. Spectral, or time series, analysis enables examination of the frequency content of the topographic profile. Although spectral analysis originated in communication engineering, in recent years it has been applied to other fields, including analysis of terrain roughness. Suggested by Bekker (1960) as one quantitative specification of terrain roughness, it has been applied to off-road hard ground by Kozin, Cote, and Bogdanoff (1963), and to the lunar surface, as photographed by Rangers VII and VIII, by Jaeger and Schuring (1966) and Van Deusen (1966).

Techniques for the derivation of the PSD function have been investigated as part of the Geological Survey's Lunar Trafficability project, sponsored by NASA. The particular problems of analyzing a topographic profile by this method have been studied, and the PSD functions of several terrestrial and lunar topographic profiles have been determined. This report summarizes the results.

POWER SPECTRAL DENSITY FUNCTION

Definition

Profiles of lunar and analogous terrestrial topography cannot be described by a specific functional relationship; thus, for the purpose of mathematical analysis, they are random profiles. The frequency content of such profiles is determined by spectral analysis. Nearby points on these profiles can be reasonably assumed to exhibit some degree of correlation, which, expressed as a function of the distance between them, can be stated mathematically as:

$$R(v) = \frac{1}{N}\int_0^N h(x)\cdot h(x+v)\,dx, \quad |v| < N$$

where $h(x)$ and $h(x + v)$ represent "neighboring" elevations at a distance v apart, and N is the total number of elevation points considered. $R(v)$ is called the autocorrelation function.

The value of $R(v)$ for specific values of v may contain information regarding the frequency content of a specific profile. For example, consider the unlikely (and nonrandom) surface profile of figure 1. For distance $v = b$, $R(v) = 0$ for all values of x, but for $v = 2b$, $R(v) = \frac{1}{2} E^2$, since for half of the values of x, $h(x) \cdot h(x + 2b) = 0$, and for the remaining values of x, $h(x) \cdot h(x + 2b) = E^2$. The graph of the autocorrelation function (fig. 2) illustrates the presence of the frequency which has periodicity $2b$ in the surface profile.

From this very simple, nonrandom example, it is possible to extrapolate the concept of the power spectrum. The power spectrum is a measurement of the amount of variation of the profile height contributed by the various frequencies present. For the above example, only one frequency, $\frac{1}{2b}$, contributes to the variation of profile height, as can be seen from the autocorrelation function graph (fig. 2). Hence, the graph of the power spectrum of this example would be a single spike representing power, $P(\omega)$, at the frequency $\frac{1}{2b}$ (fig. 3).

Determination of the power spectrum for a nonperiodic function demands a rather lengthy mathematical development, but can be explained intuitively as follows: Any periodic function can be described by its Fourier series representation; thus, the autocorrelation function of figure 2 can be represented by a Fourier series of the form $R(v) = \sum_{n=0}^{\infty} F(n) \cos n\omega v$, where $\frac{2\pi}{\omega}$ is the period of the function. If the function is nonperiodic, as is a random function, this concept can be extended by considering the periodicity to be infinite, and its representation becomes the Fourier integral over all frequencies:

$$R(v) = \frac{1}{\pi} \int_0^{\infty} P(\omega) \cos \omega v \, d\omega$$

In electrical theory, power is proportional to the square of either the voltage or the current. This term can be carried over to functions in general, and thus power is described as the mean square value of any function. If the function is periodic, the power contributed by any discrete frequency can be described as the square of the Fourier coefficient associated with the frequency. When v = 0 in the autocorrelation function, the function becomes $\frac{1}{N}\int_0^N h^2(x)dx$, which is the mean square value, or power, of h(x). Parseval's theorem then shows that the power spectrum is given by $P(n) = |F(n)|^2$.

If a random profile is considered as one in which a continuum of frequencies contribute to the variations of profile height, it becomes obvious that the power contributed can be found only for bands of frequencies, and not for discrete frequencies. Thus, we will be dealing with the power spectral density (PSD), i.e. the power per unit bandwidth, rather than the power spectrum. Since the autocorrelation function of a random profile is expressed as a Fourier integral, PSD can be shown to be equivalent to its Fourier transform, $P(\omega) = 2\int_0^\infty R(v) \cos \omega v dv$. Thus, given the autocorrelation function, the PSD function can be determined, and vice versa.

As a further illustration of the relationship of the autocorrelation and PSD functions, consider a terrain profile consisting of great amplitude differences in closely spaced points. The autocorrelation function for such a profile will show little correlation between "neighboring" points, but the PSD function will show great power in the high frequency bands.

Assumptions

Two conditions must exist before a spectral analysis can be made of any given random profile. First, the profile must represent a stationary process, i.e. its statistical properties will be unaffected by a change in the origin of the profile. This

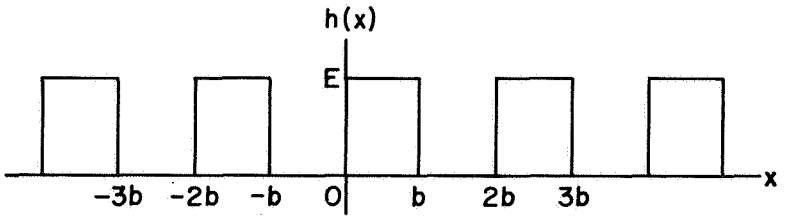

Figure 1.--Arbitrary nonrandom surface profile.

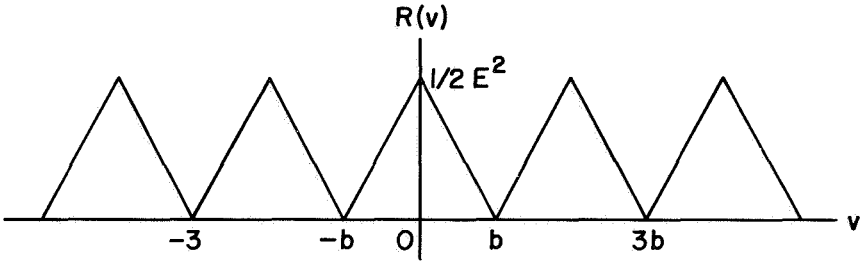

Figure 2.--Autocorrelation function of arbitrary surface in figure 1.

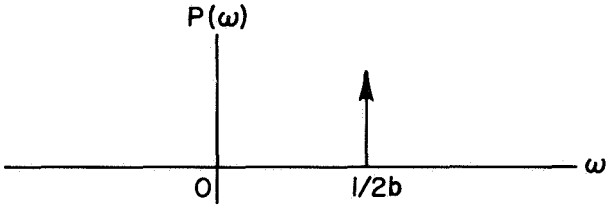

Figure 3.--Power spectrum of arbitrary surface in figure 1.

Figure 4.--Profile showing aliasing problem.

condition may be assumed to hold when a sample profile is obtained entirely within a single homogeneous terrain unit. Second, the mean value of the profile height must be zero; if it is not, it can easily be converted by normalizing the data.

Problems in Spectral Analysis

In the actual determination of the PSD function, several rather difficult problems arise. Basically, these are of two types: 1) instability in the spectral estimates resulting from sampling limitations, and 2) contamination of the "true" power spectrum by long trends in the profile.

Statistical Estimation

When a terrain profile is recorded, only a finite number of discrete data points can be obtained over a finite length. Consequently, the autocorrelation and PSD functions which are determined will of necessity be estimates of the "true" functions, as, mathematically, both are integrals over all frequencies or lags. This leads to the following problems of statistical estimation:

(1) Profile heights can be read only at discrete points, resulting in loss of information. As illustrated in figure 4, if the sampling interval is Δx, frequencies in the profile greater than $\frac{1}{2\Delta x}$ cannot be detected. However, the power found attributable to the frequency $\frac{1}{2\Delta x}$ is actually compounded by all higher frequencies which are indistinguishable from $\frac{1}{2\Delta x}$ and are multiples of it. This aliasing problem can be corrected in signals produced by electronic devices by filtering out frequencies higher than $\frac{1}{2\Delta x}$ prior to sampling the data. In terrain profiles, however, aliasing can be avoided only by choosing a sampling interval smaller than any physically expected profile frequency. This, obviously, is not usually possible, particularly when considering lunar terrain profile limitations.

(2) Since the profile record is of finite length, autocorrelation functions for large lags (the distance v between points on the profile) must be formed from very few observations. This produces a great deal of instability in the statistical

estimates of the PSD function. To correct this, statisticians have devised several lag windows (weight functions) to be applied to the autocorrelation function, or similarly, spectral windows (kernels) to be applied to the PSD function. Generally, the lag windows apply decreasing weights to increasing lags in order to decrease the sampling error incurred by including the large lags in the autocorrelation function. Unfortunately, although these windows increase the stability of the estimate of the PSD function, they also increase the bandwidth of frequencies contributing to the power. Conversely, decreasing the bandwidth of frequencies also decreases the stability of the estimates. Many reliable windows have been proposed, as well as criteria for testing them, and the merits of each have been extensively debated.

Detrending

A long-term trend affects the PSD function of a profile in two ways: 1) it may result in a nonstationary profile (i.e. a profile whose statistical properties are affected by a change in origin), and 2) since the amplitude of the profile associated with the low frequency of a long trend would likely be relatively large, enough power would be contributed by the low frequency to obscure that contributed by higher frequencies. Since the effect of low frequencies is irrelevant to vehicle response, profiles can be detrended (i.e. long trends can be eliminated) in order to more accurately describe the power in the range of frequencies which are appropriate for vehicle response.

Several methods of detrending have been proposed: linear detrending (Parzen, 1964), paraboloid fitting and linear running average (Kozin, Cote, and Bogdanoff, 1963), and an exponentially weighted average (Van Deusen, 1966). For a detrending method to be effective, the data in the frequency range which best describes the terrain roughness must remain unaltered. However, in eliminating the power contributed by low frequencies, detrending also attenuates the power at some, if not all, of the higher frequencies. The results of an investigation of this problem are discussed in the appendix.

Interpretation

PSD functions of terrain profiles are usually plotted on log-log graph paper, with frequency units of cycles per meter and power units of meters^2 per cycle per meter. Terrestrial and lunar terrain samples both possess the same general characteristics, i.e. the power contributed by lower frequencies is much greater than that contributed by higher frequencies. Van Deusen (1966) noted that, in general, PSD functions of terrain have a slope of -2 when plotted on log-log paper. There are, however, significant differences in some frequency ranges in the spectrums of the various terrain units, and the entire spectrum of one terrain may be greater than that of another by at least an order of magnitude. Thus, the roughness of one terrain sample may be much greater than another over all frequencies.

The application of spectral analysis to vehicle design is accomplished by "shaping," in an analog computer, the power spectrum of a white-noise generator (the PSD of a random function) to approximate that of the power spectrum of the terrain under consideration. A simulated terrain profile is then generated by the computer, and is subsequently used as input into a system of differential equations which describe the dynamic response of a vehicle. The analog computer simulates the physical system, and can thus provide the design specifications for the vehicle that will be best suited for terrain of a given spectral composition.

TECHNIQUES USED

In the past, scientists who have determined the PSD functions of terrains have selected various different spectral windows and have used various techniques to detrend profiles. It is doubtful whether valid comparisons of terrain roughness can be drawn from such studies. Consistent methods and techniques must be applied to all terrain units, both terrestrial and lunar, before valid comparisons can be made. Also, techniques should be used that will provide the stablest spectral estimates and that will least distort the "true" spectrum.

Spectral Window

Since data samples for a terrain profile are not continuous, finite forms of the autocorrelation and PSD functions must be used In this study the estimates suggested by Jenkins (1961) have been used:

$$R(v) = \frac{1}{N_x} \sum_{x=1}^{N-v} h'(x)h'(x+v), \quad v = 0, 1, \ldots\ldots, M$$

where

$h'(x) = h(x) - \overline{h(x)}$,

$\overline{h(x)}$ = sample mean profile height,

M = maximum lag.

$$P(\omega) = 2\Delta\left[R(0) + 2\sum_{v=1}^{M} \lambda(v)R(v) \cos \omega v\right]$$

where Δ = sampling interval

$$\text{and } \lambda(v) = \begin{cases} 1 - \frac{6v^2}{M^2} \cdot (1 - \frac{v}{M}) & 0 \leq v < \frac{M}{2}, \\ 2(1 - \frac{v}{M})^3 & \frac{M}{2} \leq v \leq M, \\ 0 & v > M \end{cases}$$

$\lambda(v)$ is the lag window suggested by Parzen (1961). This form of the PSD function $P(\omega)$ is the finite Fourier transform of the autocorrelation function.

In the results which follow, all spectral estimates have been made using a maximum lag of approximately 10 percent of the number of points in the terrain sample.

Detrending

In this study, the exponentially weighted average suggested by Van Deusen (1966, p. 57) has been used consistently to detrend the terrain profiles prior to determination of the PSD function.

The values of the profile elevations after detrending are given by

$$h_d(x) = h(x) - \frac{\sum_{n=0}^{\infty} \left[h(x + n\Delta) + h(x - n\Delta)\right] e^{-n\Delta/\lambda}}{2 \sum_{n=0}^{\infty} e^{-n\Delta/\lambda}}$$

where

$h(x)$ = original profile height,

Δ = sampling interval,

λ = arbitrary constant.

The choice of the value of λ greatly affects the amplitudes of the detrended profile. A value of $\lambda = 15$ was used consistently in detrending all terrain profiles in this study.

RESULTS

In the initial phases of this study, the only lunar data available were elevation values, computed at the Jet Propulsion Laboratory, of the terrain photographed in the last P-3 frames of the Ranger VIII and IX flights, and a topographic contour map of the Surveyor III landing site which was developed by R. M. Batson of the U.S. Geological Survey. Since there were many uncertainties as to the reliability of these data, they were used primarily as sources for exploratory investigations in detrending, maximum lag, and normality of the data distributions.

Use of the terrain data from the high-resolution Orbiter photography was anticipated for further spectral analysis of lunar topography. However, in processing the terrain data by the photoclinometric method (originally developed by Lambiotte and Taylor, 1967), difficulties developed that delayed spectral analyses of most lunar samples. To date, four reasonably reliable lunar terrain samples have been processed; this report includes their spectral analyses. The four areas were chosen on Lunar Orbiter III photographs (fig. 5) and are in Apollo site III P-9, which is just north of the Mare Cognitum region.

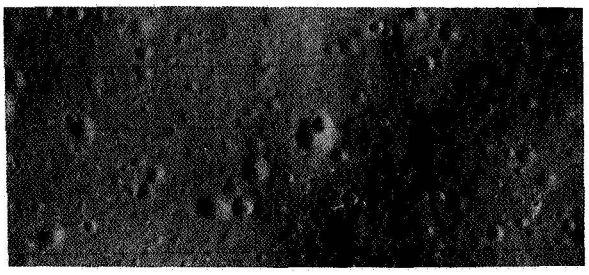

Frame H153, framelet 901

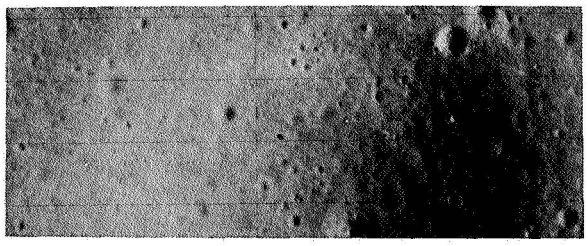

Frame H154, framelet 027 (Surveyor III landing site)

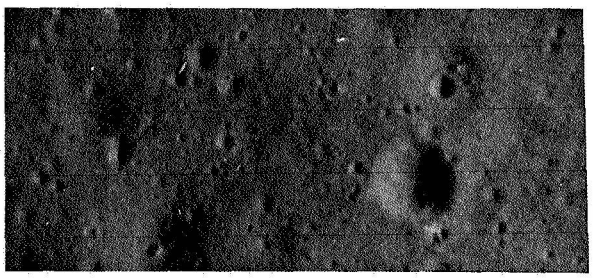

Frame H153, framelet 914

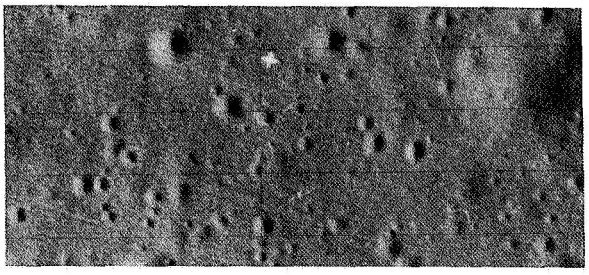

Frame H153, framelet 933

Figure 5.--Lunar terrain in four areas photographed by Lunar Orbiter III.

PSD functions have also been determined for several terrestrial terrains. These include the undisturbed terrains of the Bonito lava flow, Flagstaff, Ariz. (fig. 6; data from a contour map by R. M. Batson, U.S. Geological Survey) and of the Perth Amboy, N. J., micro-badlands (fig. 7; data from a contour map by A. Strahler, Geology Dept., Columbia Univ.). Also included are the man-distorted terrains of the Perryman Mud Course at the Aberdeen Proving Grounds, Md., and of the Yuma Proving Grounds, Ariz. (data from Kozin, Cote, and Bogdanoff, 1963).

Finally, spectral analysis has been completed on two simulated lunar terrains: the Cinder Lake crater field near Flagstaff, Ariz. (fig. 8) and the Suffield test crater "Distant Plain," near Ralston, Alberta, Canada (data from a contour map courtesy of Dr. G. H. S. Jones). All the areas, lunar and terrestrial, have been sampled at an interval of approximately 0.6 meter.

Figure 9 shows the PSD functions of the four lunar terrain profiles. These surfaces are obviously similar in degree of roughness; however, the PSD curve of the framelet 933 profile indicates slightly lower power at all frequencies.

One of the lunar PSD functions is compared with those of the undisturbed terrestrial terrains and that of the Suffield crater in figure 10. The lunar terrain appears to be much less rough than the terrestrial ones. The high power at all frequencies of both the Perth Amboy micro-badlands and the Bonito flow indicate very rough terrains, and the very high power at the high frequencies in the Bonito flow PSD function indicates the extreme roughness of the area, as any one who has observed it can attest. It is interesting to note that the PSD function values for the Suffield crater are considerably greater at all frequencies than that of the lunar surface sampled.

Figure 11 compares the PSD functions of the "smoothest" lunar terrain profile, framelet 933, with those of the man-distorted terrestrial terrains and with that of the simulated lunar mare of Cinder Lake crater field. It is striking that the simulated lunar

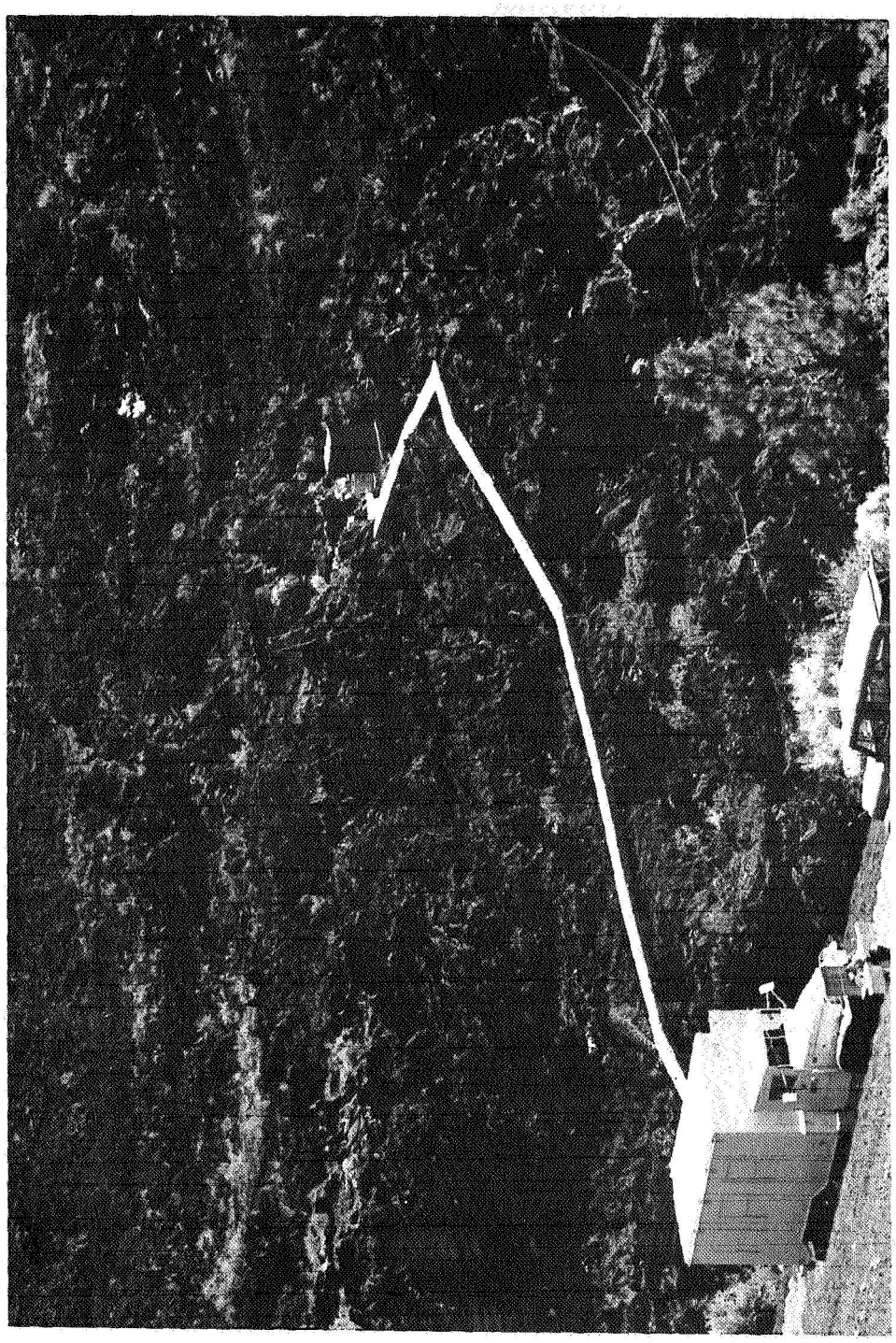

Figure 6.--Bonito lava flow, Flagstaff, Ariz.

Figure 7.--Micro-badlands topography, Perth Amboy, N. J. (courtesy of Dr. Stanley Schumm, Colorado State Univ.).

Figure 8.--Cinder Lake crater field, Flagstaff, Ariz.

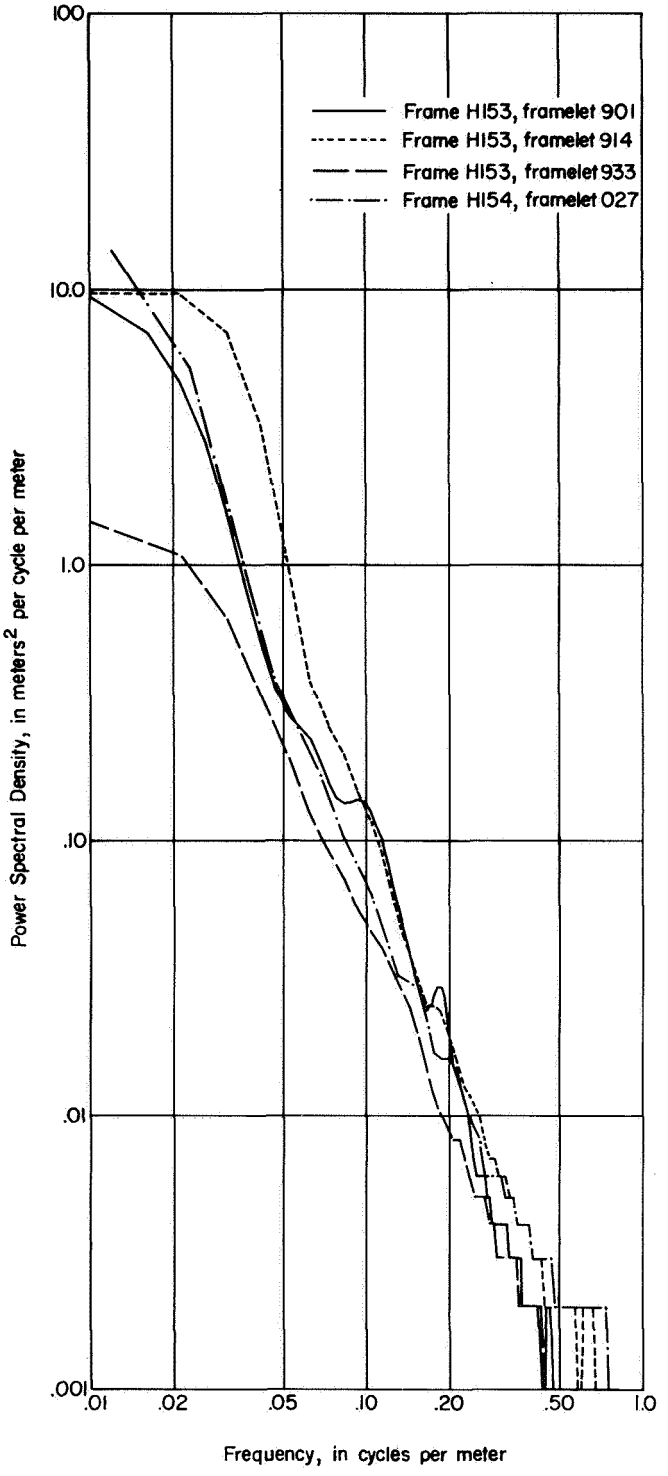

Figure 9.--Power spectral density functions of detrended lunar terrain profiles (from Lunar Orbiter III).

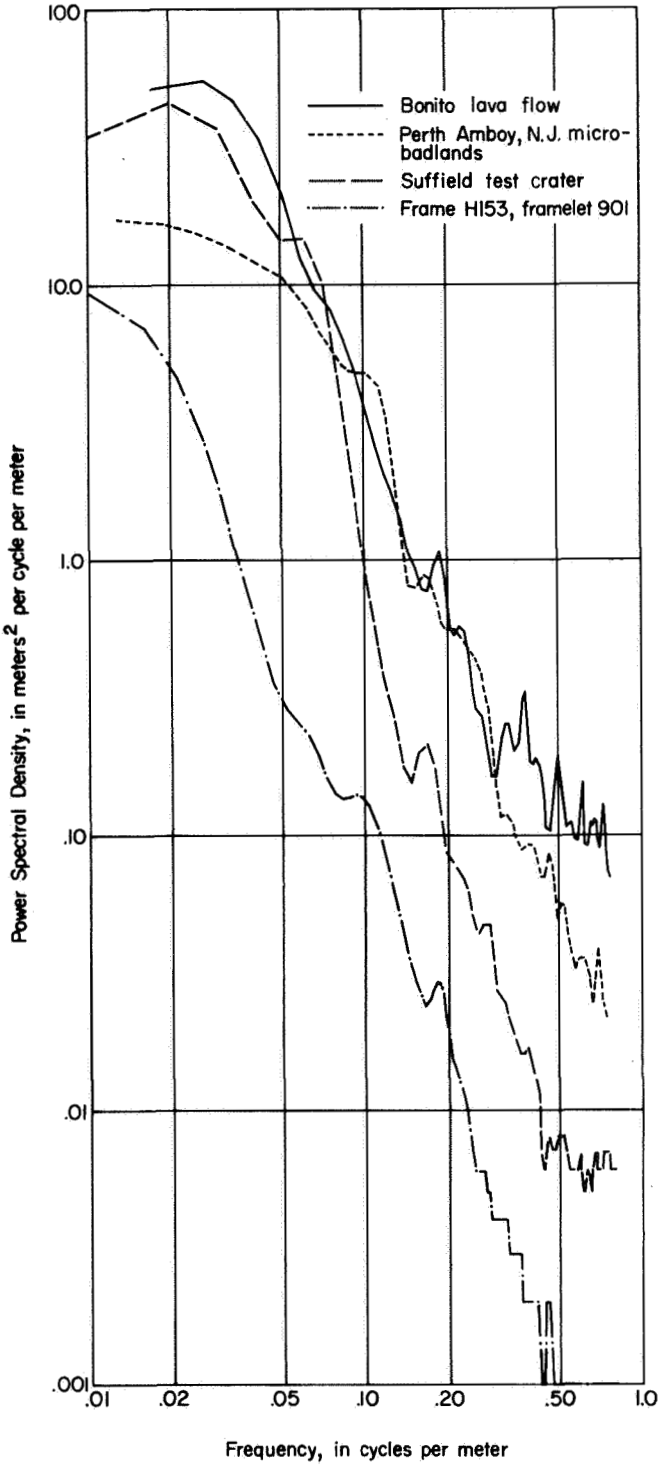

Figure 10.--Comparison of power spectral density functions of detrended lunar terrain profile with detrended undisturbed terrestrial terrain profiles.

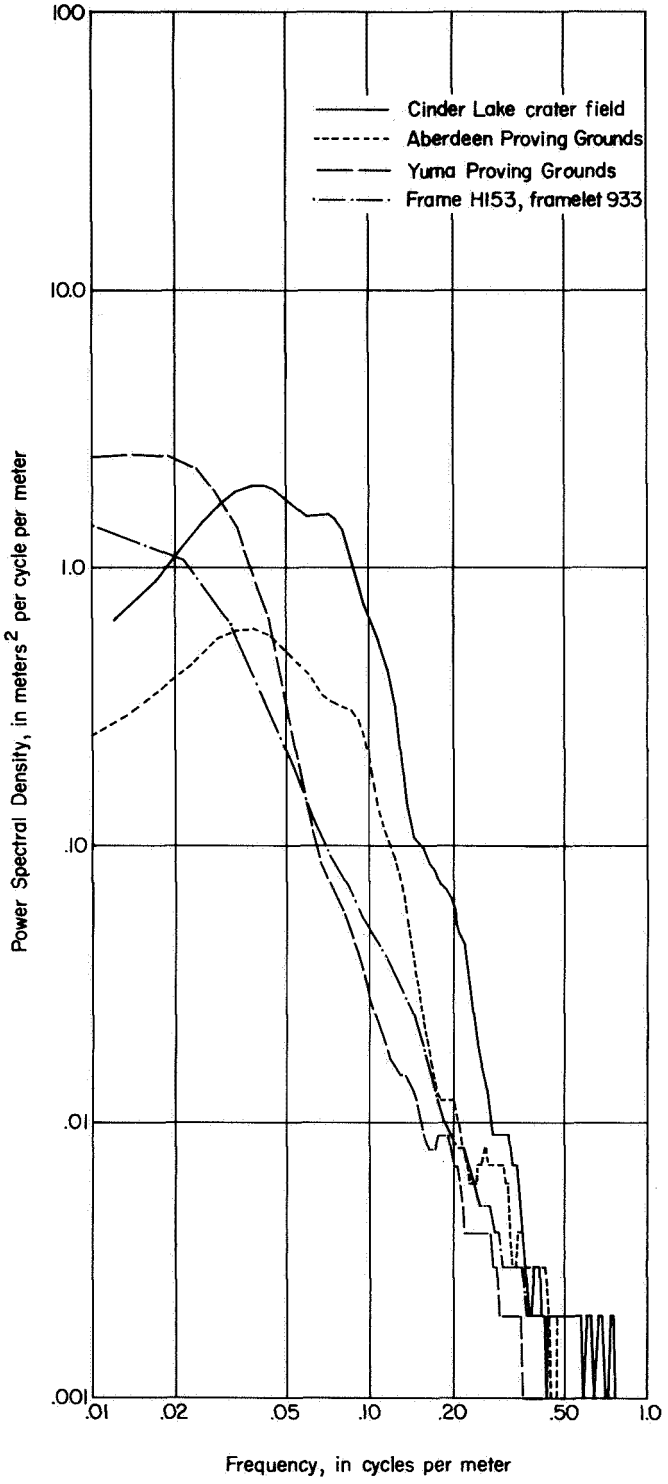

Figure 11.--Comparison of power spectral density functions of detrended lunar terrain profile with detrended man-distorted terrestrial terrain profiles.

crater field PSD function shows greater power at all frequencies than that shown by the actual lunar terrain profile. It is also noteworthy that the lunar PSD function generally indicates less roughness than the Aberdeen and Yuma Proving Grounds profiles, and that these two areas are readily trafficable by many types of vehicles.

It should be remembered that although these PSD function graphs indicate power for frequencies from 0.01 to about 0.8 cycles per meter, the frequency range considered relevant to vehicle dynamics (Jaeger and Schuring, 1966) is from 0.05 to 0.5 cycles per meter. Thus, the topographic variations affecting vehicular response have wavelengths from 2 to 20 meters.

FUTURE APPLICATIONS

The results of this study suggest that the lunar surfaces sampled are no rougher than many surfaces on Earth, and are considerably smoother than many others. Other lunar surfaces should be investigated in order to gain a more complete picture of lunar trafficability.

A very important application of spectral analysis which has not yet been attempted is in geological terrain analyses. The PSD function may be useful for description of geomorphological types and therefore of many geologic map units, as well as a statistical parameter of surface roughness.

ACKNOWLEDGMENTS

Appreciation is expressed to Dr. M. G. Bekker and Dr. Dietrich Schuring of AC Electronics, Defense Research Laboratories, for advice and technical assistance during this study. Appreciation is also given to Dr. B. D. Van Deusen of the Defense Operations Division, Chrysler Corp., for consultative advice. Finally, the writer is greatly indebted to Dr. Richard M. Jaeger of the National Center for Educational Statistics, Department of Health, Education, and Welfare, for his valuable advice and assistance during the course of this study.

REFERENCES

Bekker, M. G., 1960, Off-the-road locomotion: Ann Arbor, University of Michigan Press.

Bendat, J. S., and Piersol, A. G., 1966, Measurement and analysis of random data: New York, John Wiley and Sons, Inc., 377 p.

Blackman, R. B., and Tukey, J. W., 1958, The measurement of power spectra: New York, Dover Publications, 180 p.

Jaeger, R. M., and Schuring, D. J., 1966, Spectrum analysis of terrain of Mare Cognitum: Jour. Geophys. Research, v. 71, no. 8, p. 2023-2028.

Jenkins, G. M., 1961, General considerations in the analysis of spectra: Technometrics, v. 3, no. 2, p. 133-166.

Kozin, F., Cote, L. J., and Bogdanoff, J. L., 1963, Statistical studies of stable ground roughness: U.S. Army Tank Automotive Center, Rept. 8391, 160 p.

Lambiotte, J. J., and Taylor, G. R., 1967, A photometric technique for deriving slopes from Lunar Orbiter photography, presented at Space Systems for Planetary Geology and Geophysics Conf., Boston, 1967: Natl. Aeronautics and Space Adm., Langley Research Center, 22 p.

Lee, Y. W., 1960, Statistical theory of communication: New York, John Wiley and Sons, Inc., 501 p.

Mason, R. L., McCombs, W. M., and Cramblit, D. C., 1964, Engineering lunar model surface: Natl. Aeronautics and Space Adm., Kennedy Space Center, Rept. TR-83-D.

McCauley, J. F., 1964, Terrain analysis of the lunar equatorial belt: U.S. Geol. Survey open-file report, 44 p. [1965].

Olivier, J. R., and Valentine, R. E., 1965, Engineering lunar model obstacles: Natl. Aeronautics and Space Adm., Kennedy Space Center, Rept. TR-145-D.

Parzen, E., 1961, Mathematical considerations in the estimation of spectra: Technometrics, v. 3, no. 2, p. 167-190.

_____1964, An approach to empirical time series analysis: Radio Sci. Jour. Research, v. 68D, no. 9, p. 937-951.

Rowan, L. C., and McCauley, J. F., 1966, Lunar terrain analysis, in Lunar Orbiter--Image analysis studies report, May 1, 1965-Jan. 31, 1966: U.S. Geol. Survey open-file report, p. 89-129.

Schloss, M., 1965, Quantifying terrain roughness on lunar and planetary surfaces: AIAA Paper 65-389, AIAA 2d Ann. Mtg., San Francisco, Calif.

Van Deusen, B. D., 1966, A statistical technique for the dynamic analysis of vehicles traversing rough yielding and non-yielding surfaces: prepared for NASA under contract NASW-1287 by Advanced Projects Organization, Chrysler Corp., Detroit, Mich., 178 p.

APPENDIX

Effects of Detrending on the PSD Function

A theoretical approach was initially taken in studying the effects of detrending, following the suggestion of Van Deusen (1966, p. 57, 58) that the profile be considered as a continuous sinusoid of the form $h(x) = \sin 2\pi\omega x$. Thus, when a profile is detrended, only the amplitude is affected. The ratio of the amplitudes of the original and the detrended profiles is $\frac{1}{1 + (\frac{1}{2\pi\omega\lambda})^2}$, which is a function of both frequency (ω) and weighting constant (λ). Since power is proportional to the square of the profile amplitude, the effect of detrending on the power spectrum can be described by the transfer function, i.e., the square of the amplitude ratio. Table 1 shows the transfer function values for various values of the weighting constant (λ), and several frequency values which are relevant to vehicle response. Note that for $\lambda = 15$, the transfer function values are greater than 0.90 for all frequencies computed; thus, the power attenuation is less than 10 percent over all these frequencies.

Although this result seemed promising, the consideration that the profile data are not continuous led to the conclusion that the sampling interval might affect the transfer function values. Again using the sinusoid $h(x) = \sin 2\pi\omega x$ to describe the profile (frequency (ω) must be retained as a factor of the transfer function) but using a discrete sampling interval in the detrending equation (see page 10), the transfer function values were found to be the square of

$$1 - \frac{\sum_{n=0}^{3\lambda/\Delta} (\cos 2\pi n\omega\Delta) \cdot e^{-n\Delta/\lambda}}{\sum_{n=0}^{3\lambda/\Delta} e^{-n\Delta/\lambda}}$$

Table 2 shows the values of the transfer function for the same values of ω and λ as table 1 but for the discrete sampling interval $\Delta = 0.611$ meters. These values are consistently less than those found by considering the data to be continuous, suggesting that the attenuation in power resulting from detrending increases as the sampling interval increases. Nevertheless, for the sampling interval $\Delta = 0.611$, which is approximately the maximum resolution possible for the lunar terrain profiles, a weighting constant of $\lambda = 15$ does not cause a power attenuation of more than 10 percent except at the 0.5 frequency.

These results led to the decision to detrend the lunar and terrestrial profiles by the exponentially weighted average method, with a weighting constant of $\lambda = 15$. Because of the flexibility of the computer program eventually developed, it was decided late in the investigation to determine the PSD functions of all the undetrended profiles, as well as the detrended ones. Comparison of the PSD functions of most of the terrestrial profiles, viz, Bonito flow, Perth Amboy micro-badlands, Aberdeen Proving Grounds, and Cinder Lake crater field, showed that detrending had been successful, i.e., there was very little attenuation of power except at the very low frequencies. Table 3 gives the percentage of attenuation at various frequencies that resulted from detrending the Aberdeen Proving Grounds profile; figure 12 shows the PSD functions of the profile before and after it had been detrended. At frequencies greater than 0.10 cycles per meter, the two functions virtually coincide. However, comparison of PSD functions of the Yuma Proving Grounds and lunar profiles revealed that detrending had significantly distorted the "true" power spectrums. The attenuation of power in these profiles was very high, commonly as much as 90 percent over all frequencies (tables 4 and 5; figs. 13 and 14).

A possible explanation for the differences in the percentage of attenuation of power of the various terrains is suggested by observing the actual terrain profiles of Aberdeen Proving Grounds,

Table 1.--Transfer function values for continuous data of form $h(x) = \sin 2\pi\omega x$

λ \ ω	0.05	0.10	0.15	0.20	0.25	0.50
3	.2213	.6090	.7899	.8728	.9157	.9779
6	.6090	.8728	.9403	.9657	.9779	.9944
12	.8728	.9657	.9845	.9913	.9944	.9986
15	.9157	.9779	.9901	.9944	.9964	.9991
18	.9403	.9845	.9931	.9951	.9975	.9994

Table 2.--Transfer function values for data sampled at 0.611 meter intervals

λ \ ω	0.05	0.10	0.15	0.20	0.25	0.50
3	.1325	.5086	.6052	.7232	.7211	.7846
6	.5624	.8018	.8573	.8732	.8777	.8934
12	.8457	.9182	.9252	.9340	.9448	.9488
15	.8538	.9341	.9553	.9534	.9502	.9565
18	.9197	.9439	.9544	.9653	.9628	.9639

Table 3.--Percentage of attenuation of power resulting from detrending the Aberdeen Proving Grounds profile

For the frequency--	The percentage of attenuation is--	For the frequency--	The percentage of attenuation is--
0.0	97.0	0.379	3.0
.009	94.8	.388	6.6
.019	81.5	.398	9.4
.028	46.0	.407	8.4
.038	23.9	.417	5.5
.047	18.3	.426	2.9
.057	16.1	.436	1.4
.066	11.5	.445	3.0
.076	6.5	.455	7.6
.085	4.9	.464	6.6
.095	4.5	.473	3.0
.104	2.2	.483	1.7
.114	-.2	.492	2.0
.123	1.6	.502	6.3
.133	5.3	.511	10.4
.142	9.4	.521	3.9
.152	12.2	.530	-5.7
.161	11.1	.540	-7.9
.170	5.2	.549	-5.8
.180	.5	.559	-4.0
.189	-1.0	.568	.8
.199	-1.4	.578	3.3
.208	1.7	.587	3.4
.218	5.6	.597	5.4
.227	5.1	.606	8.2
.237	5.9	.616	10.4
.246	5.7	.625	9.6
.256	3.9	.634	8.1
.265	3.8	.644	8.1
.275	2.5	.653	8.2
.284	1.1	.663	9.1
.294	3.6	.672	12.0
.303	5.0	.682	15.3
.313	4.0	.691	16.0
.322	6.3	.701	12.5
.331	10.1	.710	9.9
.341	5.4	.720	10.7
.350	1.4	.729	9.2
.360	.6	.739	4.1
.369	1.1	.748	-.1
		.758	-.9

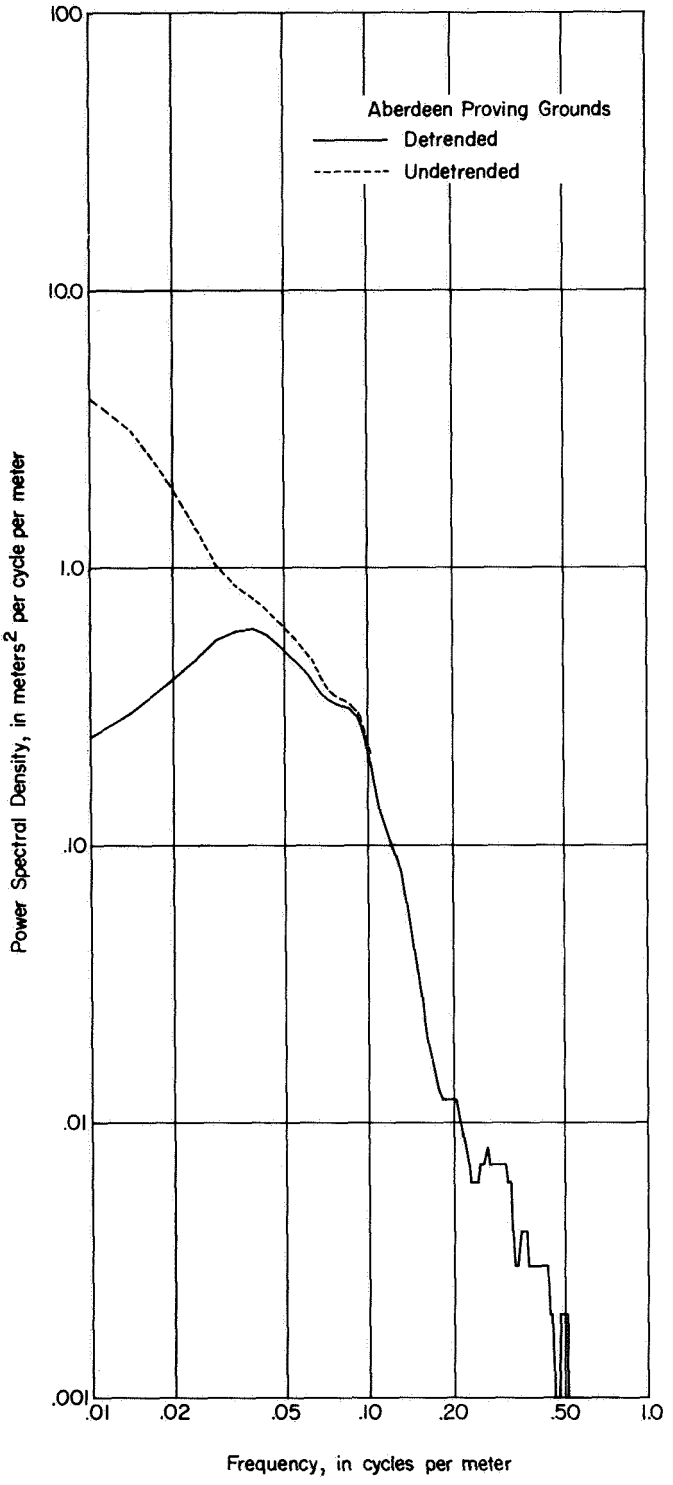

Figure 12.--Power spectral density functions of Aberdeen Proving Grounds profile before and after detrending.

Table 4.--Percentage of attenuation of power resulting from detrending the Yuma Proving Grounds profile

For the frequency--	The percentage of attenuation is--	For the frequency--	The percentage of attenuation is--
0.0	99.5	0.379	92.4
.009	99.2	.388	92.6
.019	97.1	.398	92.1
.028	82.0	.407	89.1
.038	52.0	.417	86.5
.047	72.5	.426	87.6
.057	88.7	.436	90.7
.066	83.9	.445	91.9
.076	75.3	.455	93.6
.085	81.2	.464	94.6
.095	88.3	.473	94.6
.104	85.9	.483	93.3
.114	85.0	.492	91.4
.123	87.9	.502	90.7
.133	89.9	.511	91.6
.142	88.3	.521	92.6
.152	88.1	.530	93.6
.161	88.8	.540	94.0
.170	88.0	.549	94.4
.180	83.4	.559	92.7
.189	81.4	.568	90.0
.199	83.9	.578	89.7
.208	88.0	.587	91.4
.218	89.2	.597	92.0
.227	88.2	.606	91.1
.237	86.4	.616	90.6
.246	86.0	.625	89.2
.256	85.4	.634	86.8
.265	86.1	.644	82.4
.275	88.0	.653	80.9
.284	90.5	.663	83.3
.294	91.2	.672	87.1
.303	89.4	.682	90.7
.313	87.9	.691	92.5
.322	87.5	.701	91.8
.331	87.2	.710	91.0
.341	89.0	.720	89.5
.350	91.9	.729	86.8
.360	93.0	.739	84.3
.369	92.6	.748	84.6
		.758	86.5

Table 5.--Percentage of attenuation of power resulting from detrending the Lunar Orbiter III, frame H153, framelet 901 profile

For the frequency--	The percentage of attenuation is--	For the frequency--	The percentage of attenuation is--
0.0	99.4	0.417	94.8
.010	99.3	.427	95.5
.021	98.8	.438	95.7
.031	96.0	.448	94.7
.042	87.8	.458	93.9
.052	93.4	.469	94.3
.063	95.4	.479	95.6
.073	91.3	.490	95.5
.083	84.1	.500	95.5
.094	84.4	.510	95.5
.104	86.9	.521	95.6
.115	82.3	.531	95.3
.125	81.2	.542	95.0
.135	86.3	.552	95.0
.146	90.0	.563	95.2
.156	88.4	.573	95.4
.167	87.0	.583	95.6
.177	85.7	.594	95.4
.188	85.5	.604	95.6
.198	85.3	.615	95.6
.208	87.6	.625	95.6
.219	89.0	.635	95.5
.229	90.2	.646	95.2
.240	90.7	.656	95.3
.250	91.8	.667	95.4
.260	92.1	.677	96.1
.271	92.5	.688	96.1
.281	92.6	.698	96.1
.292	93.1	.708	95.7
.302	93.3	.719	95.6
.313	93.2	.729	95.3
.323	92.6	.740	95.0
.333	92.5	.750	95.5
.344	93.0	.760	96.1
.354	93.3	.771	95.5
.365	93.6	.781	95.6
.375	94.1	.792	95.6
.385	94.4	.802	95.6
.396	94.7	.813	95.9
.406	94.5	.823	96.3
		.833	96.8

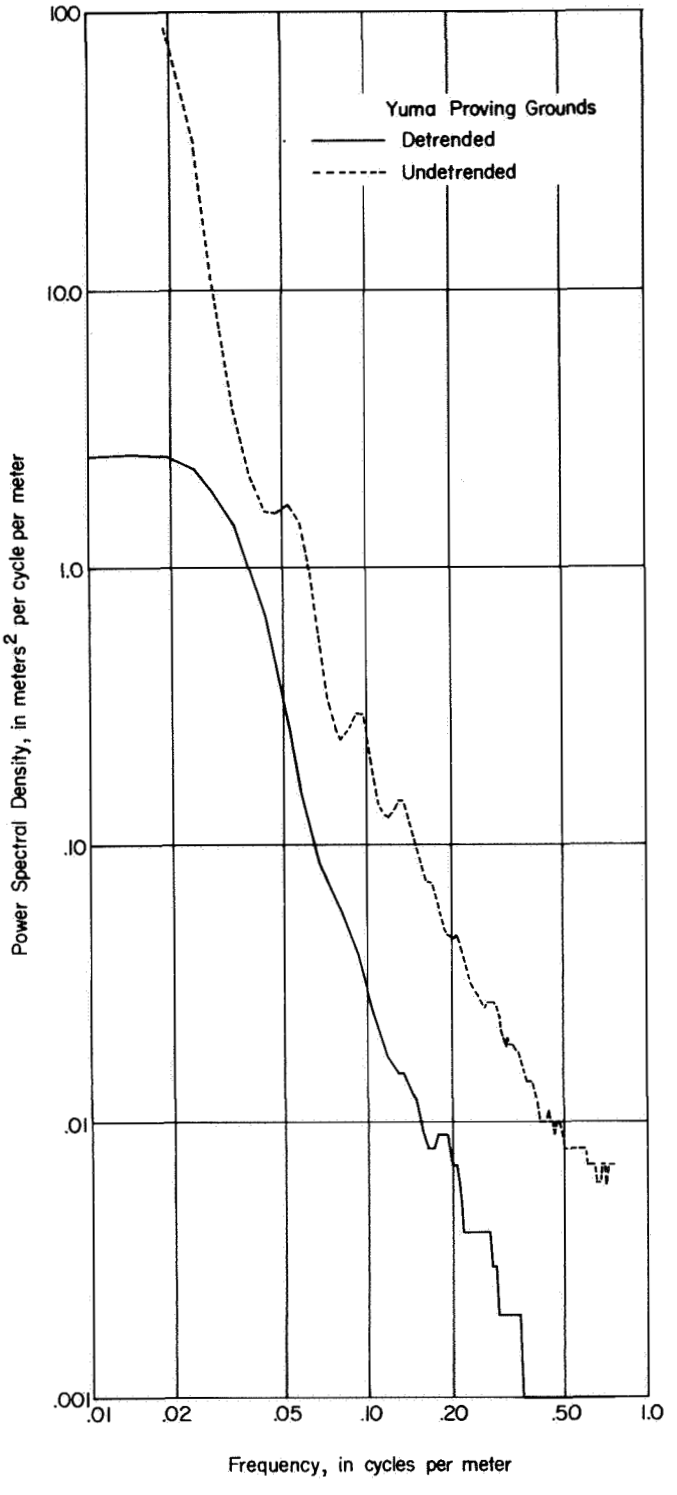

Figure 13.--Power spectral density functions of Yuma Proving Grounds profile before and after detrending.

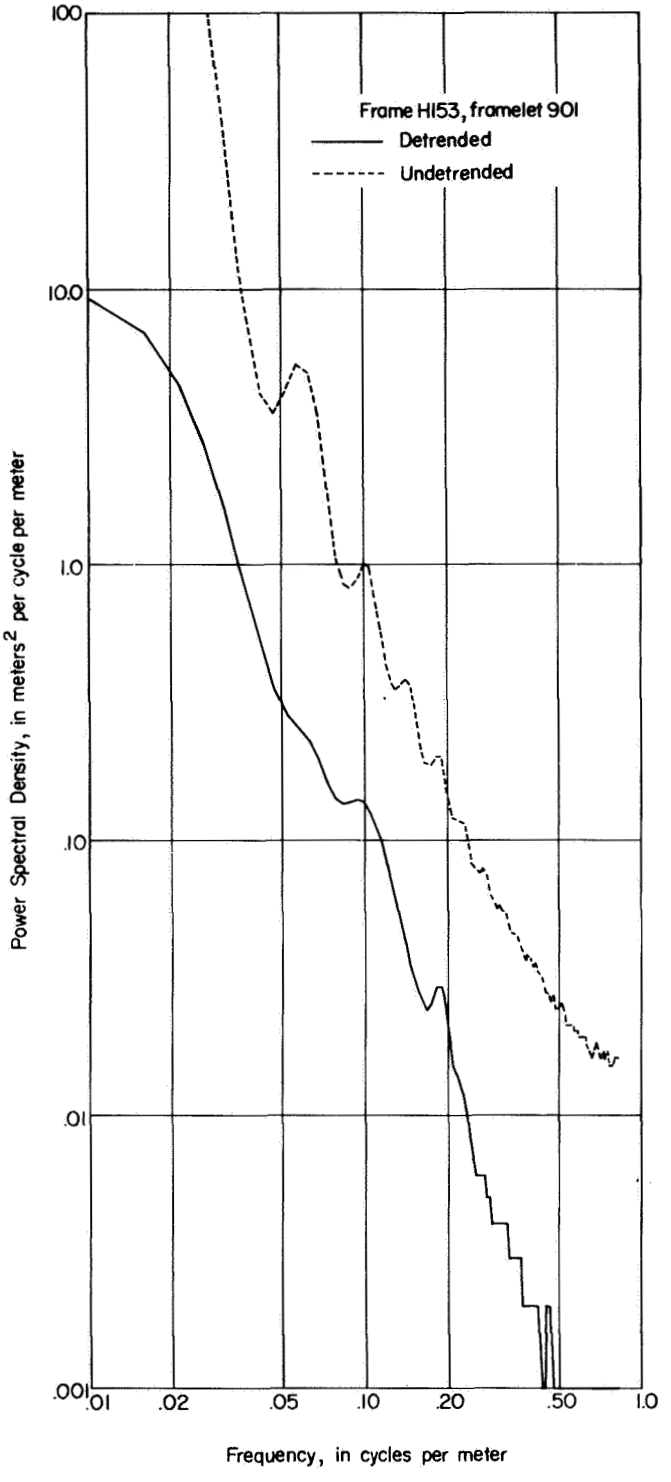

Figure 14.--Power spectral density functions of Lunar Orbiter III, frame H153, framelet 901 profile before and after detrending.

Yuma Proving Grounds, and Orbiter III, frame H153, framelet 901 (see figs. 15-17). An intuitive conclusion might be that for profiles having little or no long trends (i.e. frequencies less than 0.02 cycles per meter) the power attenuation caused by detrending is very small, whereas for profiles having significant long trends (e.g. Yuma Proving Grounds and lunar terrain) the power attenuation caused by detrending is great over all frequencies of the spectrum. Incidentally, comparison of the detrended topographic profiles (not shown in this report) with the original profiles (figs. 15-17), shows that the high frequency content of the latter is adequately preserved in the former, even for the Yuma and lunar profiles.

The bearing that the preceding observations might have on deciding whether or not to detrend a terrain profile, or on the reliability of the exponentially weighted average method of detrending, is not yet certain. For purposes of terrain analysis, detrending will probably be unnecessary.

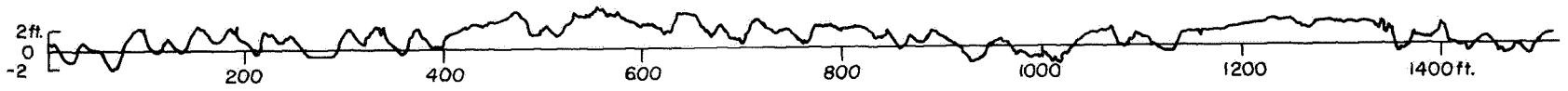

Figure 15.--Topographic profile of terrain of Aberdeen Proving Grounds, Md. Vertical : horizontal = 10:1. From Kozin, Cote, and Bogdanoff (1963); reproduced with permission of U.S. Army Tank Automotive Center.

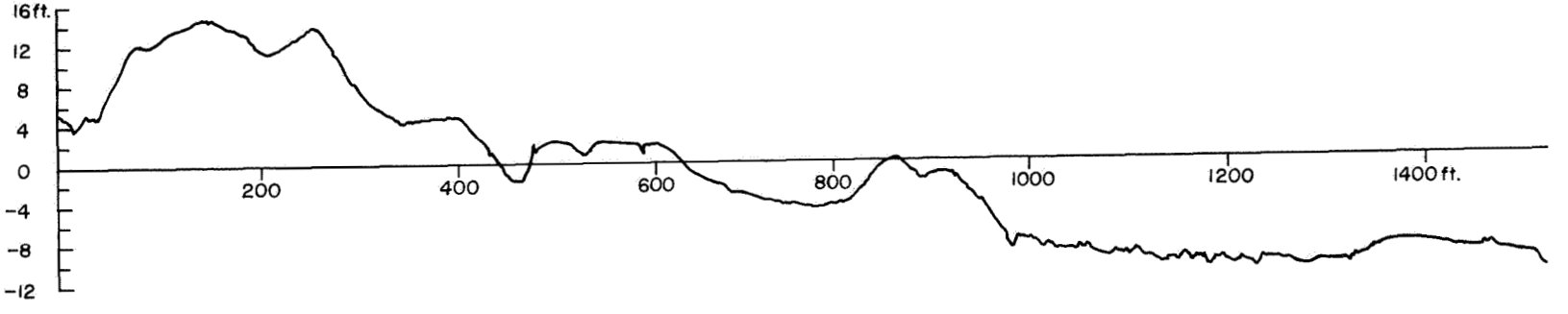

Figure 16.--Topographic profile of terrain of Yuma Proving Grounds, Ariz. Vertical : horizontal = 10:1. From Kozin, Cote, and Bogdanoff (1963); reproduced with permission of U.S. Army Tank Automotive Center.

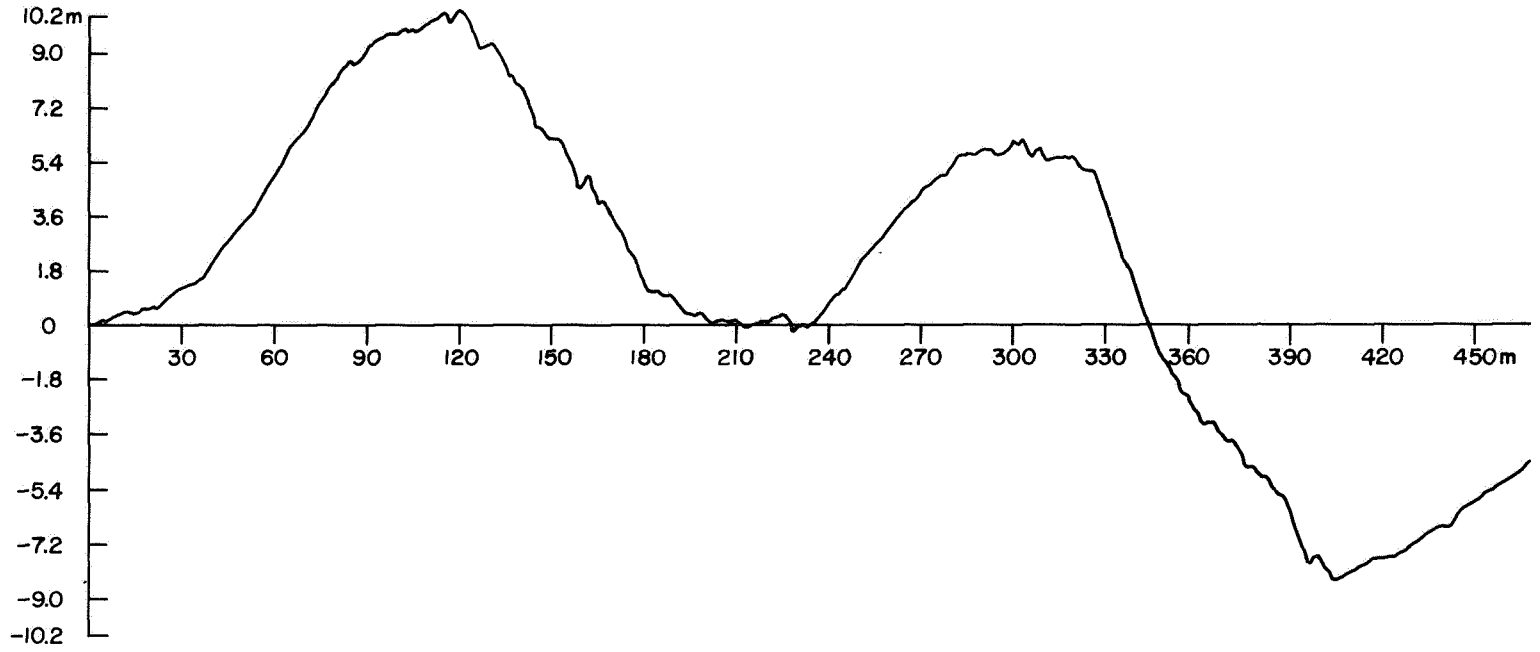

Figure 17.--Topographic profile of lunar terrain, Lunar Orbiter III, frame H153, framelet 901. Vertical : horizontal = 10.1.